INTERNATIONAL JOURNAL FOR NUMERICAL METHODS IN ENGINEERING, VOL. 33, 1269–1287 (1992)

THE DUAL BOUNDARY ELEMENT METHOD: EFFECTIVE IMPLEMENTATION FOR CRACK PROBLEMS

A. PORTELA AND M. H. ALIABADI

Wessex Institute of Technology, Computational Mechanics Institute, Ashurst Lodge, Ashurst, Southampton SO4 2AA, U.K.

D. P. ROOKE

Royal Aerospace Establishment, Farnborough, Hants GU14 6TD, U.K.

SUMMARY

The present paper is concerned with the effective numerical implementation of the two-dimensional dual boundary element method, for linear elastic crack problems. The dual equations of the method are the displacement and the traction boundary integral equations. When the displacement equation is applied on one of the crack surfaces and the traction equation on the other, general mixed-mode crack problems can be solved with a single-region formulation. Both crack surfaces are discretized with discontinuous quadratic boundary elements; this strategy not only automatically satisfies the necessary conditions for the existence of the finite-part integrals, which occur naturally, but also circumvents the problem of collocation at crack tips, crack kinks and crack-edge corners. Examples of geometries with edge, and embedded crack are analysed with the present method. Highly accurate results are obtained, when the stress intensity factor is evaluated with the J-integral technique. The accuracy and efficiency of the implementation described herein make this formulation ideal for the study of crack growth problems under mixed-mode conditions.

INTRODUCTION

The boundary element method (BEM) is a well established numerical technique in the engineering community, see Brebbia and Dominguez.[1] Its formulation in elastostatics can be based either on Betti's reciprocity theorem,[2] or simply based on the classical work theorem.[3] In both cases, a single boundary integral equation is obtained. The BEM has been successfully applied to linear elastic problems in domains containing no degenerated geometries. These degeneracies, either internal or edge surfaces which include no area or volume and across which the displacement field is discontinuous, are defined as mathematical cracks. For symmetric crack problems only one side of the crack need be modelled and a single-region BEM analysis may be used. However, in a single-region analysis, the solution of general crack problems cannot be achieved with the direct application of the BEM, because the coincidence of the crack surfaces gives rise to a singular system of algebraic equations. The equations for a point located at one of the surfaces of the crack are identical to those equations for the point, with the same co-ordinates, but on the opposite surface, because the same integral equation is collocated with the same integration path, at both coincident points.

Some special techniques have been devised to overcome this difficulty. Among these the most important are: the crack Green's function method,[4] the displacement discontinuity method,[5] the subregions method,[6] and the dual boundary element method.[7] The crack Green's function

0029–5981/92/081269–19$09.50

Received 20 December 1990
Revised 23 May 1991

method, which eliminates the need for discretization of the crack, is limited to problems with a single straight traction-free crack. Its generalization to multiple-crack problems introduces subregions to separate each individual crack, see Kuhn.[8] The displacement discontinuity method, where the unknown functions are the displacement differences between the crack surfaces, can be used directly. However, the use of derivatives in the formulation introduces higher order singularities into the boundary integrals, see Sladek *et al.*[9] and Cruse.[10] The subregions method introduces artificial boundaries into the body, which connect the cracks to the boundary, in such a way that the domain is divided into subregions without cracks. The main drawback of this method is that the introduction of artificial boundaries is not unique, and thus cannot be easily implemented into an automatic procedure. In addition, the method generates a larger system of algebraic equations than is strictly required. Despite these drawbacks, the subregions method has been the most widely used technique for crack problems.

The use of dual integral equations in crack problems was first reported by Bueckner.[11] In the boundary element method, dual equations were first presented by Watson,[12] in a formulation based on the displacement equation and its normal derivative. The theoretical bases of the dual boundary element method (DBEM) were presented by Hong and Chen,[7] in a general formulation which incorporates the displacement and the traction boundary integral equations. General mixed-mode crack problems can be solved with the DBEM, in a single-region formulation, when the displacement boundary integral equation is applied on one of the crack surfaces and the traction boundary integral equation on the other. Although the integration path is still the same for coincident points on the crack surfaces, the respective boundary integral equations are now distinct. Dual boundary element equations have been applied to solve problems in three-dimensional potential theory by Gray,[13] and in three-dimensional elastostatics by Gray *et al.*[14] An essential ingredient of both these formulations is the analytic evaluation of the singular integrals that arise from the normal derivative boundary integral equation. This feature required a special integration path around the singular point, which can be troublesome. Furthermore, the extension to edge crack problems was not dealt with in their formulation. Dual boundary element equations have also been applied to two-dimensional problems. In elastostatics Watson[12] presented results for an embedded crack problem. In potential theory, Rudolphi *et al.*[15] presented results exhibiting unexplained oscillations. Thus, there is a clear need for an alternative crack modelling strategy for the analysis of general crack problems.

The present paper is concerned with the effective numerical implementation of the two-dimensional DBEM, for solving general linear elastic fracture mechanics problems. The dual boundary integral equations are presented, the crack modelling discussed and the finite-part integrals defined. At the source point, in the traction boundary integral equation, the requirement of continuity of both the tractions and the strains implies that discretization of a crack is best done with discontinuous quadratic boundary elements. In addition, the problem of collocation at crack tips, crack kinks and crack-edge corners is automatically circumvented by the use of discontinuous elements. The effective treatment of the improper integrals of the dual equations is a matter of fundamental importance in the DBEM. For curved boundary elements, the natural definition of ordinary finite-part integrals is applied to regularize the improper integrals. For flat boundary elements, analytic integration is carried out.

The use of the standard rigid body condition, to obtain indirectly the diagonal terms of the algebraic equations at crack nodes, is no longer possible because of the existence of symmetric terms in the integrations on the opposite elements. Finally, the stress intensity factor is introduced in terms of displacement extrapolations, as well as the J-integral, and numerical results are obtained for several edge and internal cracked geometries. It is demonstrated that the present modelling strategy can be used for solving general crack problems accurately and efficiently.

THE DUAL BOUNDARY INTEGRAL EQUATIONS

The dual equations, on which the DBEM is based, are the displacement and the traction boundary integral equations. The presentation of the boundary integral equations follows Cruse.[16] In the absence of body forces, the boundary integral representation of the displacement components u_i, at an internal point $\mathbf{X}'$, is given by

$$u_i(\mathbf{X}') + \int_\Gamma T_{ij}(\mathbf{X}', \mathbf{x})u_j(\mathbf{x})\mathrm{d}\Gamma(\mathbf{x}) = \int_\Gamma U_{ij}(\mathbf{X}', \mathbf{x})t_j(\mathbf{x})\mathrm{d}\Gamma(\mathbf{x}) \tag{1}$$

where i and j denote Cartesian components; $T_{ij}(\mathbf{X}', \mathbf{x})$ and $U_{ij}(\mathbf{X}', \mathbf{x})$ represent the Kelvin traction and displacement fundamental solutions, respectively, at a boundary point $\mathbf{x}$. The distance between the points $\mathbf{X}'$ and $\mathbf{x}$ is denoted by r. The integrals in equation (1) are regular, provided $r \neq 0$. As the internal point approaches the boundary, that is as $\mathbf{X}' \to \mathbf{x}'$, the distance r tends to zero and, in the limit, the fundamental solutions exhibit singularities; they are a strong singularity of order $1/r$ in T_{ij} and a weak singularity of order $\ln 1/r$ in U_{ij}. Assuming continuity of the displacements at $\mathbf{x}'$, this limiting process produces, in the first integral of equation (1), a jump term on the displacement components and an improper integral. For a boundary point, equation (1) can now be written as

$$c_{ij}(\mathbf{x}')u_j(\mathbf{x}') + \cancel{\int}_\Gamma T_{ij}(\mathbf{x}', \mathbf{x})u_j(\mathbf{x})\mathrm{d}\Gamma(\mathbf{x}) = \int_\Gamma U_{ij}(\mathbf{x}', \mathbf{x})t_j(\mathbf{x})\mathrm{d}\Gamma(\mathbf{x}) \tag{2}$$

where $\cancel{\int}$ stands for the Cauchy principal-value integral, and the coefficient $c_{ij}(\mathbf{x}')$ is given by $\delta_{ij}/2$ for a smooth boundary at the point $\mathbf{x}'$ (δ_{ij} is the Kronecker delta).

In the absence of body forces, the stress components σ_{ij} are obtained by differentiation of equation (1), followed by the application of Hooke's law; they are given by

$$\sigma_{ij}(\mathbf{X}') + \int_\Gamma S_{ijk}(\mathbf{X}', \mathbf{x})u_k(\mathbf{x})\mathrm{d}\Gamma(\mathbf{x}) = \int_\Gamma D_{ijk}(\mathbf{X}', \mathbf{x})t_k(\mathbf{x})\mathrm{d}\Gamma(\mathbf{x}) \tag{3}$$

In this equation, $S_{ijk}(\mathbf{X}', \mathbf{x})$ and $D_{ijk}(\mathbf{X}', \mathbf{x})$ are linear combinations of derivatives of $T_{ij}(\mathbf{X}', \mathbf{x})$ and $U_{ij}(\mathbf{X}', \mathbf{x})$, respectively. The integrals in equation (3) are regular, provided $r \neq 0$. As the internal point approaches the boundary, that is as $\mathbf{X}' \to \mathbf{x}'$, the distance r tends to zero and S_{ijk} exhibits a hypersingularity of the order $1/r^2$, while D_{ijk} exhibits a strong singularity of the order $1/r$. Assuming continuity of both strains and tractions at $\mathbf{x}'$, the limiting process produces improper integrals and jump terms in strains and tractions, in the first and second integrals of equation (3), respectively. For a point on a smooth boundary, these jump terms are equivalent to boundary stresses. Hence, equation (3) can now be written as

$$\frac{1}{2}\sigma_{ij}(\mathbf{x}') + \cancel{\cancel{\int}}_\Gamma S_{ijk}(\mathbf{x}', \mathbf{x})u_k(\mathbf{x})\mathrm{d}\Gamma(\mathbf{x}) = \cancel{\int}_\Gamma D_{ijk}(\mathbf{x}', \mathbf{x})t_k(\mathbf{x})\mathrm{d}\Gamma(\mathbf{x}) \tag{4}$$

where $\cancel{\cancel{\int}}$ stands for the Hadamard[17] principal value integral. On a smooth boundary, the traction components, t_j, are given by

$$\frac{1}{2}t_j(\mathbf{x}') + n_i(\mathbf{x}')\cancel{\cancel{\int}}_\Gamma S_{ijk}(\mathbf{x}', \mathbf{x})u_k(\mathbf{x})\mathrm{d}\Gamma(\mathbf{x}) = n_i(\mathbf{x}')\cancel{\int}_\Gamma D_{ijk}(\mathbf{x}', \mathbf{x})t_k(\mathbf{x})\mathrm{d}\Gamma(\mathbf{x}) \tag{5}$$

where n_i denotes the ith component of the unit outward normal to the boundary, at the point $\mathbf{x}'$.

Equations (2) and (5) constitute the basis of the DBEM. On a traction-free crack, these equations are simplified; the displacement and the traction equations are given by

$$c_{ij}(\mathbf{x}')u_j(\mathbf{x}') + \int\!\!\!\!\!\!-_{\Gamma_c} T_{ij}(\mathbf{x}', \mathbf{x})u_j(\mathbf{x})\,d\Gamma(\mathbf{x}) = 0 \tag{6}$$

and

$$n_i(\mathbf{x}') \int\!\!\!\!\!\!=_{\Gamma_c} S_{ijk}(\mathbf{x}', \mathbf{x})u_k(\mathbf{x})\,d\Gamma(\mathbf{x}) = 0 \tag{7}$$

respectively, where Γ_c denotes the crack boundary.

Both Cauchy and Hadamard principal-value integrals are finite parts of improper integrals, see Kutt[18] and Linz.[19] Integral representations, involving improper or divergent integrals in terms of finite-part integrals, have been used before in fracture mechanics, see Bueckner[11] and Ioakimidis.[20]

CRACK MODELLING STRATEGY

The necessary conditions for the existence of principal-value integrals, assumed in the derivation of the dual boundary integral equations, impose special restrictions on the crack modelling. Consider that both the geometry and boundary field variables are described by a piece-wise continuously differentiable approximation. Thus, the Cauchy and Hadamard principal-value integrals are equivalent to finite-part integrals of first and second order, respectively. Some basic definitions of finite-part integrals, in the context of the DBEM, are presented in Reference 21.

Consider that collocation is always done at the boundary element nodes. Under this circumstance, the finite-part integral of first order, in the displacement equation (6), requires continuity of the displacement components at the nodes: any continuous or discontinuous boundary element satisfies this requirement. In the traction equation (7), the finite-part integral of second order requires continuity of the displacement derivatives at the nodes, on a smooth boundary: discontinuous quadratic boundary elements implicitly have the necessary smoothness, since the nodes are internal points of the element. It is important to realize that if the element approximation does not satisfy these necessary continuity requirements then the finite-part integrals do not exist and spurious results can be expected from the computations.

For the sake of efficiency and to keep the simplicity of the standard boundary elements, the present formulation uses discontinuous quadratic elements for the crack modelling, as shown in Figure 1. The general modelling strategy developed in the present paper can be summarized as follows:

(i) the crack boundaries are modelled with discontinuous quadratic elements, as shown in Figure 1;
(ii) the displacement equation (2) is applied for collocation on one of the crack surfaces;
(iii) the traction equation (5) is applied for collocation on the opposite surface;
(iv) continuous quadratic elements are used along the remaining boundary of the body, except at the intersection between a crack and an edge, where discontinuous or semi-discontinuous elements are required on the edge in order to avoid a common node at the intersection, see Figure 1.

This simple strategy is robust and allows the DBEM to effectively model general edge- or embedded-crack problems; crack tips, crack-edge corners and crack kinks do not require special treatment, since they are not located at nodal points where the collocation is carried out. Other

alternatives to discontinuous elements can be used to model the crack, but they are not as efficient. For instance, Hermitian boundary elements, see Watson,[12] and Overhouser boundary elements, see Walters *et al.*,[22] also suit the continuity requirements. However, they are not readily suitable to deal with edge-crack and kinked-crack problems, as further analysis is required to consider continuity conditions at corners and kinks; in addition, they require more extensive programming.

TREATMENT OF FINITE-PART INTEGRALS

The improper integrals, that arise in the dual integral equations, are easily handled by the classical singularity-subtraction method, which leads to the natural definition of ordinary finite-part integrals. In the vicinity of a collocation node the regular part of the integrand is expressed as a Taylor's expansion. If a sufficient number of terms of the expansion are subtracted from the regular part of the integrand and then added back, the singularity can be isolated. The original improper integral is thus transformed into the sum of a regular integral and an integral of the singular function. This latter integral is then evaluated analytically, while standard Gaussian quadrature is used for numerical integration of the regular integral. The procedure is general and applicable to any type of boundary element, in which the necessary conditions for the existence of the finite-part integrals are implicitly satisfied. See Reference 21 for basic definitions of finite-part integrals, in the context of the DBEM.

Consider a discontinuous quadratic boundary element of general shape, Γ_e, that contains the collocation node. The local parametric co-ordinate ξ is defined, as usual, in the range $-1 \leqslant \xi \leqslant +1$ and the collocation node ξ' is mapped onto $\mathbf{x}'$, via the continuous element shape functions. The displacement components, u_j, are approximated in the local co-ordinate by means of the nodal values, u_j^n, and the discontinuous element shape functions. The first-order finite-part integral of equation (6) can be expressed in the local co-ordinate as

$$\oint_{\Gamma_e} T_{ij}(\mathbf{x}', \mathbf{x}) u_j(\mathbf{x}) \mathrm{d}\Gamma(\mathbf{x}) = u_j^n \oint_{-1}^{+1} \frac{f_{ij}^n(\xi)}{\xi - \xi'} \mathrm{d}\xi \tag{8}$$

where $f_{ij}^n(\xi)$ is a regular function, given by the product of the fundamental solution, a shape function and the Jacobian of the co-ordinate transformation, multiplied by the term $\xi - \xi'$. The

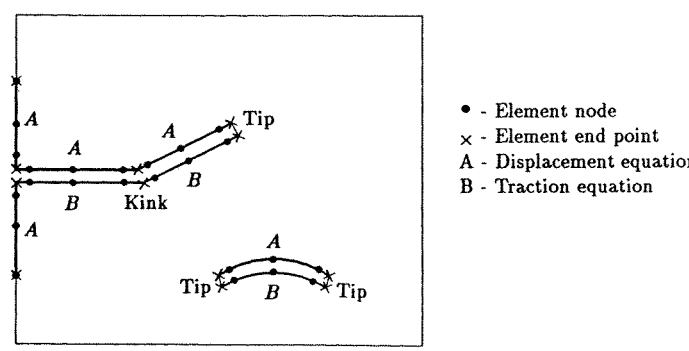

Figure 1. Crack modelling with discontinuous quadratic boundary elements

integral of the right hand side of equation (8) can be transformed with the aid of the first term of a Taylor's expansion of the function f_{ij}^n, around the collocation node, to give

$$\int_{-1}^{+1} \frac{f_{ij}^n(\xi)}{\xi - \xi'} \, d\xi = \int_{-1}^{+1} \frac{f_{ij}^n(\xi) - f_{ij}^n(\xi')}{\xi - \xi'} \, d\xi + f_{ij}^n(\xi') \int_{-1}^{+1} \frac{d\xi}{\xi - \xi'} \tag{9}$$

Now, the first integral of the right hand side is regular and the second one can be integrated analytically to give

$$\int_{-1}^{+1} \frac{d\xi}{\xi - \xi'} = \ln \left| \frac{1 - \xi'}{1 + \xi'} \right| \tag{10}$$

In equation (9), the existence of the finite-part integral requires the Hölder continuity of f_{ij}^n, at the collocation node. For the discontinuous element, this requirement is automatically satisfied, because the nodes are internal points of the element, where f_{ij}^n is continuously differentiable. The second order finite-part integral of equation (7) can be expressed in the local parametric co-ordinate as

$$\int_{\Gamma_e} S_{ijk}(\mathbf{x}', \mathbf{x}) u_k(\mathbf{x}) d\Gamma(\mathbf{x}) = u_k^n \int_{-1}^{+1} \frac{g_{ijk}^n(\xi)}{(\xi - \xi')^2} \, d\xi \tag{11}$$

where $g_{ijk}^n(\xi)$ is a regular function, given by the product of the fundamental solution, a shape function and the Jacobian of the co-ordinate transformation, multiplied by the term $(\xi - \xi')^2$. The integral on the right hand side of equation (11) can be transformed with the aid of the first and second terms of a Taylor's expansion of the density function g_{ijk}^n, in the neighbourhood of the collocation node, to

$$\begin{aligned} \int_{-1}^{+1} \frac{g_{ijk}^n(\xi)}{(\xi - \xi')^2} \, d\xi = & \int_{-1}^{+1} \frac{g_{ijk}^n(\xi) - g_{ijk}^n(\xi') - g_{ijk}^{n(1)}(\xi')(\xi - \xi')}{(\xi - \xi')^2} \, d\xi \\ & + g_{ijk}^n(\xi') \int_{-1}^{+1} \frac{d\xi}{(\xi - \xi')^2} \\ & + g_{ijk}^{n(1)}(\xi') \int_{-1}^{+1} \frac{d\xi}{\xi - \xi'} \end{aligned} \tag{12}$$

where $g_{ijk}^{n(1)}$ denotes the first derivative of g_{ijk}^n. At the collocation node the function g_{ijk}^n is required to have continuity of its second derivative or, at least, a Hölder-continuous first derivative, for the finite-part integrals to exist. This requirement is automatically satisfied by the discontinuous element, since the nodes are internal points of the element. Now, in equation (12), the first integral on the right hand side is regular and the third integral is identical with the one given in equation (10). The second integral on the right hand side of equation (12) can be integrated analytically to give

$$\int_{-1}^{+1} \frac{d\xi}{(\xi - \xi')^2} = -\frac{1}{1 + \xi'} - \frac{1}{1 - \xi'} \tag{13}$$

Equations (9) and (12) are the ordinary double-sided first- and second-order finite-part integrals respectively, as defined by Kutt.[18]

In many practical problems the cracks are flat; but cracks do grow along curved paths which are usually modelled as piece-wise flat. For piece-wise flat cracks, all the integrals in equations (9) and (12) are most effectively carried out by direct analytic integration, which is presented in the

following. Consider a flat discontinuous quadratic boundary element, with the nodes positioned arbitrarily at the points $\xi = -\frac{2}{3}$, $\xi = 0$ and $\xi = +\frac{2}{3}$. The shape functions of this element are given by

$$N_1 = \xi\left(\frac{9}{8}\xi - \frac{3}{4}\right)$$

$$N_2 = \left(1 - \frac{3}{2}\xi\right)\left(1 + \frac{3}{2}\xi\right)$$

$$N_3 = \xi\left(\frac{9}{8}\xi + \frac{3}{4}\right)$$

For this element, the integral of equation (6) is represented by

$$\int\!\!\!\!\!\!-_{\Gamma_e} T_{ij}(\mathbf{x}', \mathbf{x})u_j(\mathbf{x})\mathrm{d}\Gamma(\mathbf{x}) = u_j^n \int\!\!\!\!\!\!-_{-1}^{+1} T_{ij}(\xi', \mathbf{x}(\xi))N_n(\xi)J(\xi)\mathrm{d}\xi = \mathbf{h}_i^n \mathbf{u}^n \tag{14}$$

where $\mathbf{u}^n$ denotes the nodal displacement components and $J(\xi)$ is the Jacobian of the co-ordinate transformation. Because of the assumed flatness of the element, $J = l/2$, where l represents the element length and the matrix $\mathbf{h}^n$ is given by

$$\mathbf{h}^n = \frac{1 - 2\nu}{4\pi(1 - \nu)}\begin{bmatrix} 0 & -1 \\ +1 & 0 \end{bmatrix} \int\!\!\!\!\!\!-_{-1}^{+1} \frac{N_n}{\xi - \xi'}\,\mathrm{d}\xi \tag{15}$$

The first-order finite-part integrals are integrated analytically to give

$$\int\!\!\!\!\!\!-_{-1}^{+1} \frac{N_1}{\xi - \xi'}\,\mathrm{d}\xi = \frac{3}{4}\left(\frac{\xi'(3\xi' - 2)}{2}\ln\left|\frac{1 - \xi'}{1 + \xi'}\right| + 3\xi' - 2\right) \tag{16}$$

$$\int\!\!\!\!\!\!-_{-1}^{+1} \frac{N_2}{\xi - \xi'}\,\mathrm{d}\xi = \frac{1}{2}\left(\frac{(3\xi' - 2)(3\xi' + 2)}{2}\ln\left|\frac{1 + \xi'}{1 - \xi'}\right| - 9\xi'\right) \tag{17}$$

and

$$\int\!\!\!\!\!\!-_{-1}^{+1} \frac{N_3}{\xi - \xi'}\,\mathrm{d}\xi = \frac{3}{4}\left(\frac{\xi'(3\xi' + 2)}{2}\ln\left|\frac{1 - \xi'}{1 + \xi'}\right| + 3\xi' + 2\right) \tag{18}$$

The integral of equation (7) is represented by

$$=\!\!\!\!\!\!\int_{\Gamma_e} S_{ijk}(\mathbf{x}', \mathbf{x})u_k(\mathbf{x})\mathrm{d}\Gamma(\mathbf{x}) = u_k^n =\!\!\!\!\!\!\int_{-1}^{+1} S_{ijk}(\xi', \mathbf{x}(\xi))N_n(\xi)J(\xi)\mathrm{d}\xi = \bar{\mathbf{h}}_{ij}^n \mathbf{u}^n \tag{19}$$

where the matrix $\bar{\mathbf{h}}^n$ is given by

$$\bar{\mathbf{h}}^n = \frac{E}{4\pi(1 - \nu^2)}\frac{2}{l}\mathbf{S}' =\!\!\!\!\!\!\int_{-1}^{+1} \frac{\mathbf{N}_n}{(\xi - \xi')^2}\,\mathrm{d}\xi \tag{20}$$

The matrix $\mathbf{S}'$ is given by

$$\mathbf{S}' = \begin{bmatrix} +n_1(2n_2^2 + 1) & -n_2(-2n_2^2 + 1) \\ +n_1(2n_1^2 - 1) & -n_2(-2n_1^2 - 1) \\ -n_2(2n_1^2 - 1) & +n_1(-2n_2^2 + 1) \end{bmatrix} \tag{21}$$

where n_1 and n_2 are the components of the unit outward normal to the element. The second-order finite-part integrals of equation (20) are integrated analytically to give

$$\oint_{-1}^{+1} \frac{N_1}{(\xi - \xi')^2} \, d\xi = \frac{3}{4}\left((3\xi' - 1)\ln\left|\frac{1 - \xi'}{1 + \xi'}\right| + \frac{6\xi'^2 - 2\xi' - 3}{\xi'^2 - 1}\right) \tag{22}$$

$$\oint_{-1}^{+1} \frac{N_2}{(\xi - \xi')^2} \, d\xi = \frac{1}{2}\left(9\xi' \ln\left|\frac{1 + \xi'}{1 - \xi'}\right| - \frac{18\xi'^2 - 13}{\xi'^2 - 1}\right) \tag{23}$$

and

$$\oint_{-1}^{+1} \frac{N_3}{(\xi - \xi')^2} \, d\xi = \frac{3}{4}\left((3\xi' + 1)\ln\left|\frac{1 - \xi'}{1 + \xi'}\right| + \frac{6\xi'^2 + 2\xi' - 3}{\xi'^2 - 1}\right) \tag{24}$$

Equation (20) shows that the terms of the matrix $\bar{\mathbf{h}}^n$ are inversely proportional to the element length, l. This property is computationally advantageous because it can lead to diagonally dominant systems of algebraic equations. This is an obvious advantage of the present method, over the methods that use a regularized version of the traction equation.

THE RIGID BODY CONDITION

When collocation is performed at a crack node there are always two elements, on opposite faces, that contain the collocation point, because both crack surfaces are discretized. This means that, along the crack, the finite-part integrals in equations (6) and (7) are required twice: once on the element that contains the collocation node, that is the self-point element, and again, on the opposite element, which is also a self-point element, since it contains the node which is coincident with the collocation node. This peculiar feature of the DBEM puts restrictions on the use of the standard rigid body condition to indirectly evaluate diagonal terms at crack nodes, as explained in the following. Consider a constant displacement field, with components $u_i(\mathbf{x}) = C$, defined throughout the body. In this circumstance the traction components are zero and equation (2) gives

$$c_{ij}(\mathbf{x}') + \oint_{\Gamma} T_{ij}(\mathbf{x}', \mathbf{x}) d\Gamma(\mathbf{x}) = 0 \tag{25}$$

while equation (5) gives

$$n_i(\mathbf{x}') \oint_{\Gamma} S_{ijk}(\mathbf{x}', \mathbf{x}) d\Gamma(\mathbf{x}) = 0 \tag{26}$$

Equations (25) and (26) express the usual rigid body condition that must be satisfied by the dual boundary integral equations at every collocation point. According to equation (25), the coefficient $c_{ij}(\mathbf{x}')$ need not be dealt with directly. When the equation is discretized, this coefficient, together with the finite-part integral, is determined by the *row sum* technique. However, for collocation at a crack node, the *row sum* technique can no longer be used if the integration along opposite self-point elements has any symmetric terms (equal in magnitude but opposite in sign), since they will cancel each other in the sum. It can be shown, through equations (14) to (18), that the off-diagonal terms of the first and last nodes of the elements used here are symmetric, with the finite-part integrals given by (ln 5 − 3) and (− ln 5 + 3), respectively. Bearing in mind that opposite self-point elements have their first and last nodes interchanged, it is evident that two symmetric off-diagonal terms are obtained from the collocation at either one of these nodes and integration along opposite self-point elements. According to equation (26), it appears that the *row*

sum technique can be used to evaluate indirectly the diagonal terms of the discretized form of the traction equation. Again, it can be shown, through equations (19) to (24), that the diagonal terms of any crack node are symmetric with respect to its opposite node. These features invalidate the use of the standard rigid body condition, expressed in equations (25) and (26), to indirectly evaluate diagonal terms at crack nodes.

THE STRESS INTENSITY FACTOR EVALUATION

The different techniques used in the boundary element method for the evaluation of stress intensity factors are described by Aliabadi and Rooke.[23] Near-tip displacement extrapolation and J-integral methods were used to obtain the numerical results of the next section.

In the neighbourhood of the crack tip, the elastic field is defined by an infinite series expansion that can be decoupled into mode I and II components.[24] At the crack tip, the first term of the stress series is singular, while the remaining terms give zero stresses. Let r, θ be a polar co-ordinate system, centred at the crack tip, such that $\theta = \pm \pi$ defines the crack surfaces. Considering only the first term of the Williams' expansion, the displacement field on the crack surfaces can be written as

$$u_2(\theta = \pi) - u_2(\theta = -\pi) = \frac{\kappa + 1}{\mu} K_{\mathrm{I}} \sqrt{\frac{r}{2\pi}} \tag{27}$$

and

$$u_1(\theta = \pi) - u_1(\theta = -\pi) = \frac{\kappa + 1}{\mu} K_{\mathrm{II}} \sqrt{\frac{r}{2\pi}} \tag{28}$$

where μ is the shear modulus and $\kappa = 3 - 4\eta$; for plane strain $\eta = \nu$ and for plane stress $\eta = \nu/(1 + \nu)$, where ν is the Poisson's ratio. The constants K_{I} and K_{II} are the stress intensity factors for the deformation modes I and II, respectively. They can be computed from equations (27) and (28), when the displacements on the crack surfaces are known from a boundary element solution. Consider flat discontinuous quadratic boundary elements, with the non-central nodes located arbitrarily at internal points distant $l/6$ from the end points (the results were found to be insensitive to the position of the non-central nodes), in which l denotes the element length. The two opposite elements that share the crack tip are represented in Figure 2. Using equations (27)

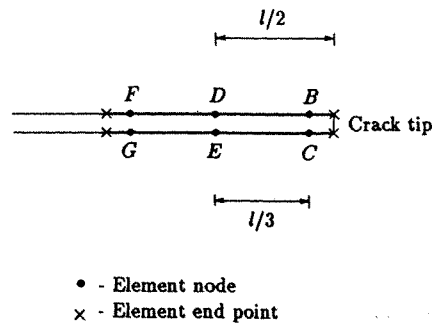

Figure 2. Crack-tip boundary elements

and (28), the stress intensity factors, evaluated with the displacements of the nodes D – E and F – G, are given by

$$K_{\mathrm{I}}^{\mathrm{DE}} = (u_2^{\mathrm{D}} - u_2^{\mathrm{E}}) \frac{\mu}{\kappa + 1} 2\sqrt{\frac{\pi}{l}} \tag{29}$$

$$K_{\mathrm{II}}^{\mathrm{DE}} = (u_1^{\mathrm{D}} - u_1^{\mathrm{E}}) \frac{\mu}{\kappa + 1} 2\sqrt{\frac{\pi}{l}} \tag{30}$$

and

$$K_{\mathrm{I}}^{\mathrm{FG}} = (u_2^{\mathrm{F}} - u_2^{\mathrm{G}}) \frac{\mu}{\kappa + 1} 2\sqrt{\frac{3\pi}{5l}} \tag{31}$$

$$K_{\mathrm{II}}^{\mathrm{FG}} = (u_1^{\mathrm{F}} - u_1^{\mathrm{G}}) \frac{\mu}{\kappa + 1} 2\sqrt{\frac{3\pi}{5l}} \tag{32}$$

respectively. By means of a linear extrapolation, from the nodes D – E and F – G to the crack tip, the stress intensity factors can be evaluated by

$$K_{\mathrm{I}} = \left[5(u_2^{\mathrm{D}} - u_2^{E}) - \frac{3\sqrt{15}}{5} (u_2^{\mathrm{F}} - u_2^{\mathrm{G}}) \right] \frac{\mu}{\kappa + 1} \sqrt{\frac{\pi}{l}} \tag{33}$$

and

$$K_{\mathrm{II}} = \left[5(u_1^{\mathrm{D}} - u_1^{\mathrm{E}}) - \frac{3\sqrt{15}}{5} (u_1^{\mathrm{F}} - u_1^{\mathrm{G}}) \right] \frac{\mu}{\kappa + 1} \sqrt{\frac{\pi}{l}} \tag{34}$$

Equations (29) and (30), along with equations (33) and (34), are the ones used for the computation of the stress intensity factors, presented in the next section.

The J-integral is an effective method for the determination of stress intensity factors, because the elastic field can be accurately determined, with the boundary element method. Consider a Cartesian reference system, defined at the tip of a traction-free crack, as shown in Figure 3. Neglecting the body forces, Rice[25] introduced the path-independent J-integral; the rate of energy released per unit of crack translation in the x_k direction is defined as

$$J_k = \int_{\Gamma} (W n_k - t_j u_{j,k}) \mathrm{d}\Gamma \tag{35}$$

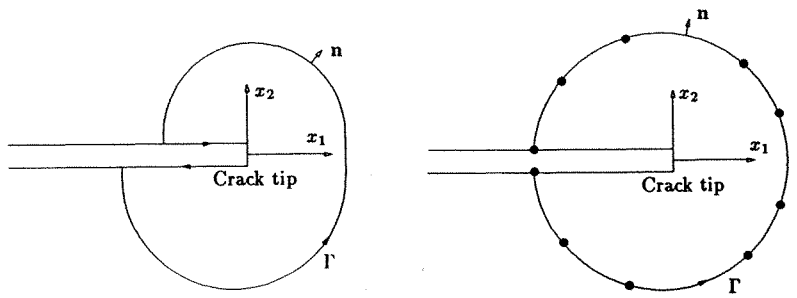

Figure 3. Co-ordinate reference system and contour path for J-integral

in which Γ is an arbitrary contour surrounding the crack tip; W is the strain energy density, $W = \frac{1}{2}\sigma_{ij}\varepsilon_{ij}$, where σ_{ij} and ε_{ij} are the stress and strain tensors, respectively; t_j are the traction components, defined along the contour, $t_j = \sigma_{ij}n_i$, where n_i are the components of the unit outward normal to the contour path. The relations between the components of the J-integral and the stress intensity factors are given by

$$J_1 = \frac{K_{\mathrm{I}}^2 + K_{\mathrm{II}}^2}{E'} \tag{36}$$

and

$$J_2 = -\frac{2K_{\mathrm{I}}K_{\mathrm{II}}}{E'} \tag{37}$$

where the constants E' is the elasticity modulus E for plane stress conditions and $E' = E/(1 - \nu^2)$ for plane strain conditions. Application of equations (36) and (37) to mixed-mode crack problems has been limited owing to difficulties in decoupling the mode I and mode II stress intensity factors from the J-integral components. However, a simple procedure based on the decomposition of the elastic field into its respective symmetric and antisymmetric mode components, can be used to decouple the stress intensity factors of a mixed-mode problem. This procedure was first presented by Kitagawa *et al.*[26] and used in the boundary element method by Aliabadi.[27] The integral J_1 is represented by the sum of two integrals as follows:

$$J_1 = J_1^{\mathrm{I}} + J_1^{\mathrm{II}} \tag{38}$$

where the superscripts indicate the pertinent deformation mode. For this representation to be possible, it is sufficient to introduce the following decomposition in the elastic fields:

$$\begin{Bmatrix} \sigma_{11}^{\mathrm{I}} \\ \sigma_{22}^{\mathrm{I}} \\ \sigma_{12}^{\mathrm{I}} \end{Bmatrix} = \frac{1}{2}\begin{Bmatrix} \sigma_{11} + \sigma'_{11} \\ \sigma_{22} + \sigma'_{22} \\ \sigma_{12} - \sigma'_{12} \end{Bmatrix}, \quad \begin{Bmatrix} \sigma_{11}^{\mathrm{II}} \\ \sigma_{22}^{\mathrm{II}} \\ \sigma_{12}^{\mathrm{II}} \end{Bmatrix} = \frac{1}{2}\begin{Bmatrix} \sigma_{11} - \sigma'_{11} \\ \sigma_{22} - \sigma'_{22} \\ \sigma_{12} + \sigma'_{12} \end{Bmatrix} \tag{39}$$

and

$$\begin{Bmatrix} u_1^{\mathrm{I}} \\ u_2^{\mathrm{I}} \end{Bmatrix} = \frac{1}{2}\begin{Bmatrix} u_1 + u'_1 \\ u_2 - u'_2 \end{Bmatrix}, \quad \begin{Bmatrix} u_1^{\mathrm{II}} \\ u_2^{\mathrm{II}} \end{Bmatrix} = \frac{1}{2}\begin{Bmatrix} u_1 - u'_1 \\ u_2 + u'_2 \end{Bmatrix} \tag{40}$$

in which

$$\sigma'_{ij}(x_1, x_2) = \sigma_{ij}(x_1, -x_2)$$

and

$$u'_i(x_1, x_2) = u_i(x_1, -x_2)$$

Equations (39) and (40) lead to the following decompositions of the elastic field:

$$\sigma_{ij} = \sigma_{ij}^{\mathrm{I}} + \sigma_{ij}^{\mathrm{II}} \tag{41}$$

and

$$u_i = u_i^{\mathrm{I}} + u_i^{\mathrm{II}} \tag{42}$$

When equations (41) and (42) are introduced in equation (35), equation (38) is obtained, with the J-integral components given by

$$J_i^{\mathrm{M}} = \int_\Gamma (W^{\mathrm{M}} n_i - t_j^{\mathrm{M}} u_{j,i}^{\mathrm{M}}) \mathrm{d}\Gamma \tag{43}$$

for M = I or M = II. Finally, the following relations hold:

$$J_1^{\mathrm{I}} = \frac{K_{\mathrm{I}}^2}{E'}, \quad J_1^{\mathrm{II}} = \frac{K_{\mathrm{II}}^2}{E'} \tag{44}$$

The implementation of this procedure into the boundary element method is straightforward. A circular contour path, around the crack tip, is defined with a set of internal points, located at symmetrical positions, relatively to the crack plane, as shown in Figure 3. The two contour points on the crack surfaces are the first and the last points of the path respectively. In a circular path, at these points, it is always verified that $n_1 = -1, n_2 = 0$ and thus, for a traction-free crack, $t_2 = 0$. For the sake of simplicity, only circular paths containing crack nodes were considered. The integration, along the contour path, can be accomplished with the trapezoidal rule or by Gaussian quadrature.

NUMERICAL RESULTS

The results obtained with displacement extrapolations will be referred to in terms of the definitions presented in Figure 2. For the J-integral calculations, only circular paths, centred at the tip and containing a pair of crack nodes, were considered; each path is referred to by a path number which increases as the radius of the contour increases, as shown in Figure 4.

As a first test, consider a rectangular plate, with a single horizontal edge crack, represented in Figure 5. The crack length is denoted by a, the width of the plate is denoted by w and the height by $2h$. The plate is subjected to the action of a uniform traction $\bar{t}$, symmetrically applied at the ends. Results have been obtained for the cases in which $h/w = 0{\cdot}5$, in order to be compared with the results published by Civelek and Erdogan.[28] Five cases were considered, with $a/w = 0{\cdot}2$, $0{\cdot}3$, $0{\cdot}4$, $0{\cdot}5$ and $0{\cdot}6$, respectively. A convergence study was carried out with three different meshes of 32,

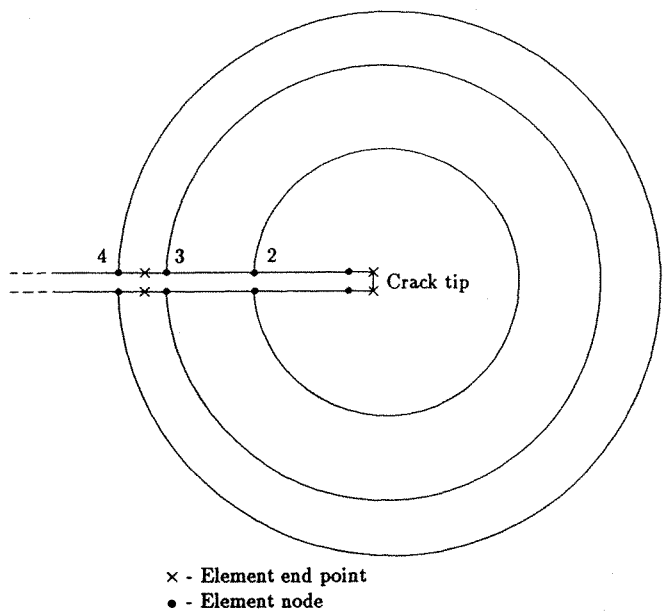

Figure 4. Circular path numbering system for J-integral contours

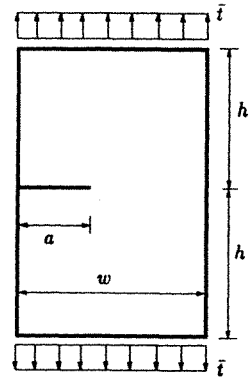

Figure 5. Rectangular plate with a single edge crack ($h/w = 0{\cdot}5$)

Table I. Stress intensity factors for a single horizontal edge crack in a rectangular plate ($h/w = 0{\cdot}5$)

	$K_I/(\bar{t}\sqrt{\pi a})$							
	Displ./extrap.		J-integral contour path					Reference
a/w	D − E	D−EF−G	2	3	4	5	8	28
0·2	1·566	1·618	1·496	1·495	1·495	1·494	1·495	1·488
0·3	1·962	2·014	1·860	1·859	1·858	1·857	1·858	1·848
0·4	2·230	2·537	2·340	2·338	2·338	2·336	2·335	2·324
0·5	3·268	3·292	3·032	3·029	3·028	3·025	3·021	3·010
0·6	4·580	4·558	4·188	4·185	4·184	4·179	4·168	4·152

40 and 64 quadratic boundary elements, in which the crack was discretized with 4, 5 and 8 quadratic discontinuous elements on each surface, respectively; convergence was achieved with the mesh of 32 elements (differences between the results of the 32 and 64 element meshes are less than 0·1 per cent), in which the crack discretization was graded, towards the tip, with the ratios 0·4, 0·3, 0·2 and 0·1. The results obtained with the mesh of 32 elements are presented in Table I. For the J-integral computations, 10 internal points and the trapezoidal rule were used. Comparing the results of the displacement extrapolations with those of Reference 28, it can be concluded that the central nodes formula D − E is more accurate than the extrapolation formula D − E F − G, with percentage differences between 4 and 10, relatively to the results of Reference 28. On the other hand, the results obtained with the J-integral show a high level of accuracy; the largest difference between these results and those of Reference 28 does not exceed 0·6 per cent. Also, notice the stability of the J-integral results, for any contour path. Figure 6 shows the initial and deformed boundary element meshes for the case $a/w = 0{\cdot}6$. Notice that, although discontinuous elements are used to model the crack surfaces, no oscillations are present in the results. This is an important feature of the present formulation that clearly differs from that reported in the work of Rudolphi *et al.*[15]

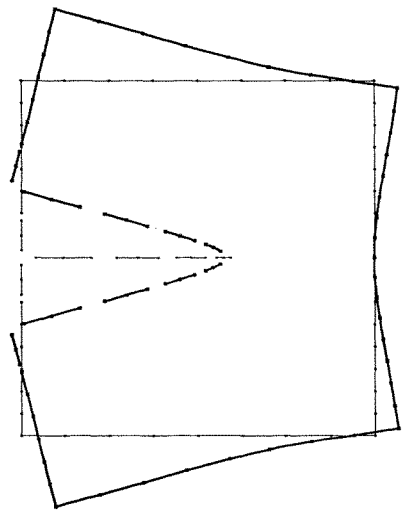

Figure 6. Initial and deformed boundary element meshes for the edge-crack problem ($a/w = 0{\cdot}6$)

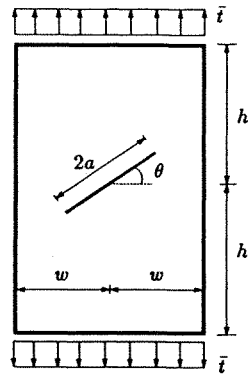

Figure 7. Rectangular plate with a central slant crack ($h/w = 2$, $\theta = 45°$)

Consider, now, the analysis of a central slant crack in a rectangular plate, represented in Figure 7. The plate is loaded with a uniform traction $\bar{t}$, symmetrically applied at the ends. The ratio between the height and the width of the plate is given by $h/w = 2$. The crack has the length $2a$ and makes an angle of $\theta = 45°$ with the horizontal direction. Accurate results for this problem were published by Murakami.[29] To solve this problem with the DBEM, a mesh of 36 quadratic boundary elements was set up, in which 6 discontinuous elements were used on each side of the crack, graded towards the tips, with the ratios 0·25, 0·15 and 0·1. The results obtained are presented in Tables II and III. The J-integral computations were carried out with 30 internal points and trapezoidal integration rule. With such a coarse mesh, the results obtained with the J-integral are remarkably accurate; the present results match those of Reference 29 within two decimal places. For mode II, the stability of the J-integral results is slightly lower than for mode I. This means that, in the deformation mode II, the variation of the elastic field along the contour

Table II. Mode I stress intensity factors for a central slant crack in a rectangular plate ($h/w = 2$, $\theta = 45°$).

	$K_I/(\bar{t}\sqrt{\pi a})$						
	Displacements	J-integral contour path					Reference
a/w	D – E	2	3	4	5	8	29
0·2	0·531	0·521	0·519	0·521	0·521	0·521	0.518
0·3	0·554	0·544	0·542	0·544	0·544	0·544	0·541
0·4	0·588	0·575	0·574	0·576	0·576	0·576	0·572
0·5	0·632	0·616	0·614	0·617	0·617	0·616	0·612
0·6	0·686	0·666	0·665	0·667	0·667	0·666	0·661

Table III. Mode II stress intensity factors for a central slant crack in a rectangular plate ($h/w = 2$, $\theta = 45°$).

	$K_{II}/(\bar{t}\sqrt{\pi a})$						
	Displacements	J-integral contour path					Reference
a/w	D – E	2	3	4	5	8	29
0·2	0·519	0·499	0·499	0·501	0·503	0·508	0·507
0·3	0·528	0·508	0·508	0·511	0·512	0·517	0·516
0·4	0·541	0·521	0·521	0·523	0·525	0·529	0·529
0·5	0·558	0·538	0·538	0·541	0·542	0·547	0·546
0·6	0·579	0·560	0·560	0·562	0·564	0·569	0·567

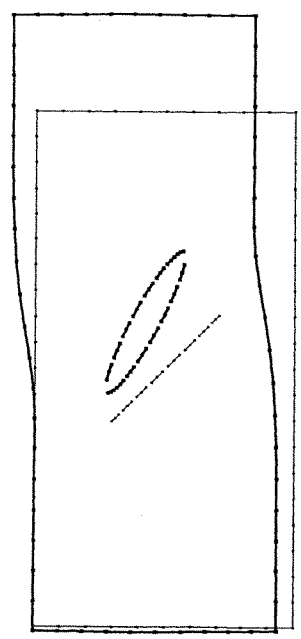

Figure 8. Initial and deformed boundary element meshes for the centre-crack problem ($a/w = 0·6$)

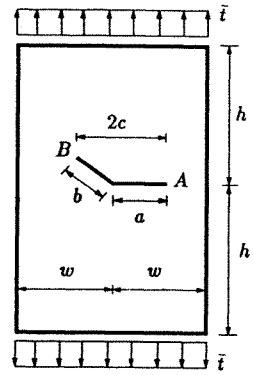

Figure 9. Rectangular plate with an internal kinked crack ($h/w = 2$, $a/w = 0{\cdot}1$)

Table IV. Mode I stress intensity factors for tip A; rectangular plate with an internal kinked crack ($h/w = 2$, $a/w = 0{\cdot}1$)

	$K_I/(\bar{t}\sqrt{\pi c})$						
	Displacements	J-integral contour path					Reference
b/a	D − E	2	3	4	5	8	29
0·2	1·021	0·998	0·995	0·997	0·996	0·993	0·995
0·4	1·018	0·993	0·990	0·992	0·991	0·989	0·990
0·6	1·017	0·990	0·987	0·989	0·988	0·987	0·986

Table V. Mode II stress intensity factors for tip A; rectangular plate with an internal kinked crack ($h/w = 2$, $a/w = 0{\cdot}1$)

	$K_{II}/(\bar{t}\sqrt{\pi c})$						
	Displacements	J-integral contour path					Reference
b/a	D − E	2	3	4	5	8	29
0·2	0·030	0·029	0·029	0·030	0·030	0·030	0·028
0·4	0·036	0·034	0·035	0·035	0·035	0·036	0·033
0·6	0·032	0·031	0·032	0·032	0·032	0·032	0·030

paths is not accurately approximated with the trapezoidal integration rule. Improved stability could easily be obtained by considering either more internal points along each path or a higher order integration rule. Figure 8 shows the initial and deformed boundary element meshes for the case $a/w = 0{\cdot}6$.

As a final test, consider the analysis of a rectangular plate, with an internal kinked crack, represented in Figure 9. One of the segments of the crack is horizontal with length a while the

Table VI. Mode I stress intensity factors for tip B; rectangular plate with an internal kinked crack ($h/w = 2$, $a/w = 0{\cdot}1$)

	$K_I/(\bar{t}\sqrt{\pi c})$						
	Displacements	J-integral contour path					Reference
b/a	D − E	2	3	4	5	8	29
0·2	0·634	0·605	0·603	0·603	0·604	0·604	0·598
0·4	0·603	0·578	0·576	0·576	0·576	0·576	0·574
0·6	0·595	0·572	0·570	0·570	0·570	0·570	0·568

Table VII. Mode II stress intensity factors for tip B; rectangular plate with an internal kinked crack ($h/w = 2$, $a/w = 0{\cdot}1$)

	$K_{II}/(\bar{t}\sqrt{\pi c})$						
	Displacements	J-integral contour path					Reference
b/a	D − E	2	3	4	5	8	29
0·2	0·589	0·556	0·556	0·555	0·555	0·556	0·557
0·4	0·637	0·602	0·602	0·601	0·602	0·603	0·607
0·6	0·659	0·623	0·623	0·623	0·623	0·624	0·627

other segment makes an angle of 45° with the horizontal and has a length b; the horizontal projection of the total crack is given by $2c = a + \sqrt{2}b/2$. The kink of the crack is at the centre of the plate, which has a height equal to twice the width and is loaded at the ends with a uniform traction $\bar{t}$. Three cases were considered, $b/a = 0{\cdot}2$, 0·4 and 0·6, with $a/w = 0{\cdot}1$. The stress intensity factors were obtained for both tips A and B, with a boundary element mesh of 48 quadratic elements, in which the horizontal and the inclined segments of the crack were discretized with 5 and 4 discontinuous quadratic elements on each crack face, respectively. The results are presented in Tables IV to VII. Accurate results for comparison are published by Murakami.[29] Again, the performance of the DBEM is excellent, when the stress intensity factors are evaluated with the J-integral. Even with the present relatively coarse mesh, the results obtained match those of Reference 29 within two decimal places.

CONCLUSIONS

The DBEM incorporates two independent boundary integral equations; one is the usual displacement boundary integral equation and the other one is the traction boundary integral equation. When the displacement equation is applied on one of the crack surfaces and the traction equation is applied on the other, general mixed-mode crack problems can be solved in a single-region formulation. The existence of the finite-part integrals of the traction equation requires continuity of the strains at the collocation node, on a smooth boundary. Because of this requirement, both crack surfaces are discretized with standard discontinuous quadratic boundary elements. In

addition, the discontinuous elements circumvent the problem of collocation at crack tips, crack kinks and crack-edge corners. The effective treatment of the hypersingular integrals that appear in the traction equation is of fundamental importance. For curved boundary elements a regularization integration formula, based on the definition of ordinary finite-part integrals, is proposed in the present paper. For flat boundary elements, the direct analytic integration is the most effective method to deal with such integrations. At a crack node, singular integrations do occur twice, once on the self-point element and again in the opposite one. This feature prevents the use of the standard rigid body condition to evaluate indirectly the diagonal terms of the algebraic equations at crack nodes. Several cracked geometries were analysed with the DBEM; accurate stress intensity factors were always obtained with the J-integral method.

REFERENCES

1. C. A. Brebbia and J. Dominguez, *Boundary Elements—An Introductory Course*, Computational Mechanics Publications, Southampton, U.K., 1989.
2. F. J. Rizzo, 'An integral equation approach to boundary value problems of classical elastostatics', *Quart. Appl. Math.*, **25**, 83–96 (1967).
3. A. Portela, 'Theoretical basis of boundary solutions for linear theory of structures', in C. A. Brebbia (ed.), *New Developments in Boundary Element Method, Proc. Second International Seminar on Recent Advances in Boundary Element Methods*, University of Southampton, 1980.
4. M. D. Snyder and T. A. Cruse, 'Boundary integral equation analysis of cracked anisotropic plates', *Int. J. Fract.*, **11**, 315–328 (1975).
5. S. L. Crouch, 'Solution of plane elasticity problems by the displacement discontinuity method', *Int. j. numer. methods eng.*, **10**, 301–342 (1976).
6. G. E. Blandford, A. R. Ingraffea and J. A. Liggett, 'Two-dimensional stress intensity factor computations using the boundary element method', *Int. j. numer. methods eng.*, **17**, 387–404 (1991).
7. H. Hong and J. Chen, 'Derivations of integral equations of elasticity', *J. Eng. Mech. ASCE*, **114**, 1028–1044 (1988).
8. G. Kuhn, 'Numerische Behandlung von Mehrfachrissen in ebenen Scheiben', *ZAMM*, **61**, 105–106 (1981).
9. V. Sladek, J. Sladek and J. Balas, 'Boundary integral formulation of crack problems', *ZAMM*, **66**, 83–94 (1986).
10. T. A. Cruse, *Boundary Element Analysis in Computational Fracture Mechanics*, Kluwer Academic Publishers, Dordrecht, 1989.
11. H. F. Bueckner, 'Field singularities and related integral representations', in G. C. Sih (ed.), *Mechanics of Fracture Vol. 1*, Nordhoff, Leyden, The Netherlands, 1973.
12. J. O. Watson, 'Hermitian cubic and singular elements for plane strain', in Banerjee and Watson (eds.), *Developments in Boundary Element Methods 4*, Elsevier Applied Science Publishers, Barking, U.K., 1986.
13. L. J. Gray, 'Boundary element method for regions with thin internal cavities', IBM Bergen Scientific Centre, Allegaten 36, 5007 Bergen, Norway, 1987.
14. L. J. Gray, L. F. Martha and A. R. Ingraffea, 'Hypersingular integrals in boundary element fracture analysis', *Int. j. numer. methods eng.*, **29**, 1135–1158 (1990).
15. T. J. Rudolphi, G. Krishnasamy, L. W. Schmerr and F. J. Rizzo, 'On the use of strongly singular integral equations for crack problems', *Proc. Boundary Elements X*, Computational Mechanics Publications, Southampton, 1988.
16. T. A. Cruse, 'Mathematical foundations of the boundary integral equation method in solid mechanics', *Report No. AFOSR-TR-77-1002*, Pratt and Whitney Aircraft Group, 1977.
17. J. Hadamard, *Lectures on Cauchy's Problem in Linear Partial Differential Equations*, New Haven, Yale University Press, 1923.
18. H. R. Kutt, 'On the numerical evaluation of finite-part integrals involving an algebraic singularity', *CSIR Special Report WISK 179*, National Research Institute for Mathematical Sciences, P.O. Box 395, Pretoria 0001, South Africa, 1975.
19. D. P. Linz, 'On the approximate computation of certain strongly singular integrals', *Computing*, **35**, 345–353 (1985).
20. N. I. Ioakimidis, 'Application of finite-part integrals to the singular integral equations of crack problems in plane and three-dimensional elasticity', *Acta Mech.*, **45**, 31–47 (1982).
21. A. Portela, M. H. Aliabadi and D. P. Rooke, 'Dual boundary element analysis of linear elastic crack problems', in *Advances in BEM for Fracture Mechanics*, Computational Mechanics Publications, Southampton, U.K., to be published.
22. H. G. Walters, J. C. Ortiz, G. S. Gipson and J. A. Brewer, 'Overhouser boundary elements in potential theory and linear elastostatics', in T. A. Cruse (ed.), *Advanced Boundary Element Methods*, Springer-Verlag, Berlin, 1988.
23. M. H. Aliabadi and D. P. Rooke, *Numerical Fracture Mechanics*, Computational Mechanical Publications, Southampton, and Kluwer Academic Publishers, Dordrecht, 1991.

24. M. L. Williams, 'Stress singularities resulting from various boundary conditions in angular corners of plates in extension', *J. Appl. Mech. ASME*, **19,** 526–528 (1952).
25. J. R. Rice, 'A path independent integral and the approximate analysis of strain concentration by notches and cracks', *J. Appl. Mech. ASME*, **35,** 379–386 (1968).
26. H. Kitagawa, H. Okamura and H. Ishikawa, 'Application of *J*-integral to mixed-mode crack problems', *Trans. JSME*, No. 760-13, 46–48 (1976); *ibid.*, No. 780-4, 52–54 (1978).
27. M. H. Aliabadi, 'Evaluation of mixed-mode stress intensity factors using the path independent *J*-integral', *Proc. Boundary Elements in Engineering XII*, Hokkaido, Japan, Computational Mechanics Publications, Southampton, U.K., 1990.
28. M. B. Civelek and F. Erdogan, 'Crack problems for a rectangular sheet and an infinite strip', *Int. J. Fract.*, **19,** 139–159 (1982).
29. Y. Murakami, *Stress Intensity Factors Handbook*, Pergamon Press, Oxford, 1987.